RESEARCH ARTICLE | JANUARY 04 2012

Photodissociation pathways and lifetimes of protonated peptides and their dimers

G. Aravind; B. Klærke; J. Rajput; Y. Toker; L. H. Andersen; A. V. Bochenkova; R. Antoine; J. Lemoine; A. Racaud; P. Dugourd

J. Chem. Phys. 136, 014307 (2012)
https://doi.org/10.1063/1.3671943

Photodissociation pathways and lifetimes of protonated peptides and their dimers

G. Aravind,[1] B. Klærke,[1] J. Rajput,[1] Y. Toker,[1] L. H. Andersen,[1,a)] A. V. Bochenkova,[2,b)] R. Antoine,[3] J. Lemoine,[4] A. Racaud,[3] and P. Dugourd[3]
[1]*Department of Physics and Astronomy, Aarhus University, DK-8000 Aarhus C, Denmark*
[2]*Chemistry Department, Moscow State University, Moscow 119991, Russia and Department of Physics and Astronomy, Aarhus University, DK-8000 Aarhus C, Denmark*
[3]*Université de Lyon, F-69622, Lyon, France and Université Lyon 1, Villeurbanne, CNRS, UMR 5579, LASIM, France*
[4]*Université de Lyon, F-69622, Lyon, France and Université Lyon 1, Villeurbanne, CNRS, UMR 5180, Sciences Analytiques, France*

(Received 28 September 2011; accepted 3 December 2011; published online 4 January 2012)

Photodissociation lifetimes and fragment channels of gas-phase, protonated YA_n (n = 1,2) peptides and their dimers were measured with 266 nm photons. The protonated monomers were found to have a fast dissociation channel with an exponential lifetime of ~200 ns while the protonated dimers show an additional slow dissociation component with a lifetime of ~2 μs. Laser power dependence measurements enabled us to ascribe the fast channel in the monomer and the slow channel in the dimer to a one-photon process, whereas the fast dimer channel is from a two-photon process. The slow (1 photon) dissociation channel in the dimer was found to result in cleavage of the H-bonds after energy transfer through these H-bonds. In general, the dissociation of these protonated peptides is non-prompt and the decay time was found to increase with the size of the peptides. Quantum RRKM calculations of the microcanonical rate constants also confirmed a statistical nature of the photodissociation processes in the dipeptide monomers and dimers. The classical RRKM expression gives a rate constant as an analytical function of the number of active vibrational modes in the system, estimated separately on the basis of the equipartition theorem. It demonstrates encouraging results in predicting fragmentation lifetimes of protonated peptides. Finally, we present the first experimental evidence for a photo-induced conversion of tyrosine-containing peptides into monocyclic aromatic hydrocarbon along with a formamide molecule both found in space. © *2012 American Institute of Physics*. [doi:10.1063/1.3671943]

I. INTRODUCTION

When a large molecule is excited, internal energy redistribution normally occurs quickly. For an IR vibrational excitation[1] one or more photons are first absorbed but the energy is rapidly redistributed over all vibrational degrees of freedom by virtue of vibrational couplings. This is known as intramolecular vibrational redistribution (IVR) (Refs. 2–4) which is assumed to occur on the ps to ns timescale.[5–7] The process results in internal energy completely randomized over all degrees of freedom and it may eventually lead to unimolecular dissociation if the energy is in excess of the threshold energy required for bond-breakage. When electronic excitations are involved, fast (fs-ps timescale) rearrangement on the excited surface may also take place eventually leading to direct dissociation (we neglect electron emission here when discussing cations only). However, large molecules normally undergo internal conversion (IC) followed by IVR before undergoing dissociation.[3] Internal conversion to the electronic ground state may be ultrafast (i.e., on the femtosecond timescale) when mediated by conical intersections. This phenomenon, also called photochemical funnels, is common in the photochemistry of polyatomic molecules, where there are a number of energetically close-lying electronic states and many nuclear degrees of freedom.[8–10] Vibrational energy flow plays an important role in the reactivity of molecules both in the gas phase and in condensed media. It redistributes energy among many degrees of freedom on a timescale faster than the breaking of an activated bond and is therefore decisive for isomerization and reaction rates by making energy available to molecular modes not initially activated.[11]

In many biological systems, it is important that excess energy is transported to the host environment before vital photo damage occurs. Peptides with aromatic chromophores undergo π-π^* transition in the UV[12,13] and hence dissociation lifetime studies are relevant to understand damage of biomolecules under harmful UV radiation.[14,15] To investigate the intrinsic biomolecular response to UV excitation we have studied the photo response of small peptides and their dimers in the gas phase. Notably, studies in the gas phase yield intrinsic molecular properties without environmental perturbations.[16–28]

While many previous experiments involved radical cations of polypeptides, we here consider protonated peptides, which might have entirely different photodissociation dynamics. We report on UV-photodissociation of gas-phase

a)Electronic mail: lha@phys.au.dk.
b)Electronic mail: anastasia.bochenkova@gmail.com.

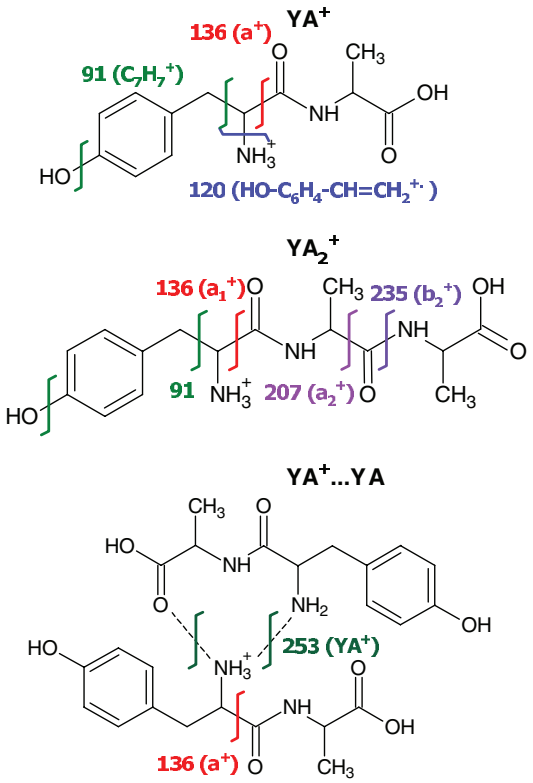

FIG. 1. Some of the peptides studied in the present work. Indicated are the cleavages that yield the dominating fragment ions shown in Fig. 9.

protonated tyrosine (Y) - alanine (A) peptide complexes, specifically, $YA_n^+[n = 1,2]$ peptide monomers and the YA dimer cation (See Fig. 1). The structure shows more than one H-bond in the dimer cation, as it is shown below. If monomers and dimers exhibit identical dissociation properties (rates and channels of dissociation) it is evident that there is (on the time scale in question) very little energy flow from the initially excited monomer to the adjacent partner peptide in the dimer system. If, on the other hand, this is not the case the two units are communicating and energy must flow from the excited monomer to the other unit, in our case through the inter-peptide H-bonds. In fact, a long dissociation time is in itself indicative of a statistical process unless energy is getting trapped, for example, in an electronically excited triplet state. We also address the variation of the microsecond and sub-microsecond dissociation lifetimes with the peptide size and discuss the fragmentation pathways. Henceforth the protonated species are merely addressed as cations.

Before we discuss the present experiment and our results we briefly mention some relevant previous studies. First, it was found that the mode of excitation of protonated peptides influences the fragmentation pattern,[20] but we find photo-excitation techniques advantageous over collisional[29] or surface-induced[30] excitation due to the well-defined excitation energy provided by the photon. It is of ultimate interest to discover whether fragmentation of large peptide cations takes place prior to IVR (Refs. 31–34) or occurs as a statistical process.[35] Weinkauf *et al.*[34] observed fast dissociation circumventing IVR in the case of polypeptide radical cations while Hu *et al.*[35] measured microcanonical rate constants for the fragmentation of $(Leu)_nTyr$ [n = 1, 2] radical cations and found them to be decreasing with increasing length of the peptide chain. In these studies, the aromatic site of the chromophore at the C-terminus was photoexcited while a unimolecular fragmentation was observed at the N-terminus yielding an iminium ion. Weinkauf *et al.*[34,36] proposed an efficient charge transfer from the excited aromatic site to the N terminus where ultra-fast fragmentation occurs. In spite of barriers, complex protein motions are also thought to cause efficient charge transfer down the peptide chain due to varying ionization potentials and dissipative degrees of freedom.[37]

As discussed by Kang *et al.*,[38] protonated tryptophan has a charge-transfer state, with $\pi\sigma^*$ character, into which an electron may be transferred from the π orbital of the indole ring. This state becomes lower than the $\pi\pi^*$ when the NH coordinate is stretched, and as a result the protonated amino acid emits a hydrogen atom on the ps time scale. It thus plays an important role in the deactivation of UV-excited amino acids in competition with internal conversion. It was later demonstrated by Wyer *et al.*[24] that the excitation wavelength is crucial for the fragmentation pattern of the protonated tyrosine-alanine dipeptide. Consequently, the 1 eV difference between a 220 nm photon and a 266 nm photon matters which perhaps is not surprising since most of the photon energy is used in the $\pi\sigma^*$ excitation. Finally, photoexcitation of small tryptophan containing peptides was recently reported[28] where fast fragmentation mechanisms on the excited states as well as slow reactions on the ground state (after IC) were discussed.

II. EXPERIMENTAL METHOD

The gas-phase peptide cations (i.e., protonated) were produced using an electrospray ion source with peptides dissolved in methanol. The ions were trapped in a Paul trap with helium buffer gas. The trapped ions were accelerated to 20 keV and mass analyzed by a magnet. The ions were guided to the interaction region after passing through a 3 degree deflector that helped avoid neutrals formed before the interaction region. The ion beam was intersected at right angle by the laser beam in the interaction region. The fourth harmonic of an Nd:YAG laser was employed in this experiment. The ion bunches were extracted at double the laser repetition rate to enable background subtraction. The neutral photofragments were detected using a micro-channel plate (MCP) detector placed 1.6 meters from the interaction region, while the ions were deflected away using an electrostatic deflector, as shown in Fig. 2. The measured quantity was the time-of-flight (TOF) of the neutral fragments formed after photo excitation.

The dissociation times were obtained by applying a uniform electric field in the interaction region.[39,40] The entrance of the field region was held at a high voltage, $V_{spec} = -2.5$ kV, with respect to the exit. The cations were thereby accelerated at the entrance of the field region and eventually decelerated back to the initial speed at the exit. The parent ions thus had varying speed along their path inside the field region and hence the neutral fragments formed have different TOF depending on their position of formation inside the field region. Thus the TOF (Fig. 3) of the neutral photofragments enabled

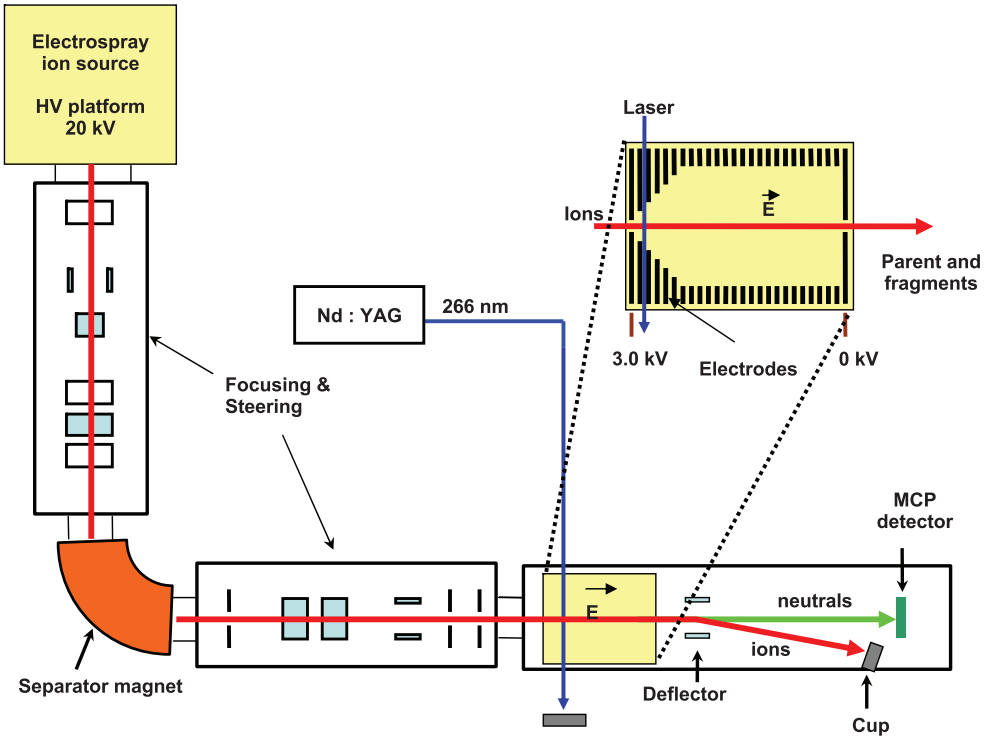

FIG. 2. Schematic representation of the experimental set-up with the ion-beam path and the laser set-up. The inset shows the spectrometer with a stack of electrodes that maintain a uniform electric field. The electric field region is about 26 cm long and the interaction region is 5 cm downstream inside the field region while the distance from the interaction spot to the MCP detector is 1.6 meters.

us to extract the sub-microsecond dissociation lifetimes. All neutral fragments formed in the 20 cm region between the exit of the field region and the ion deflector had identical TOF.

The fragment masses were identified using a modified linear quadrupole ion trap mass spectrometer (LTQ, Thermo Fisher Scientific, San Jose, CA) at Lyon University.[41] Ions produced by an electrospray-ion source were trapped and photoexcited by 5 shots of 266 nm photons. The fragment ions were mass analyzed after about 100 milliseconds of trapping time.

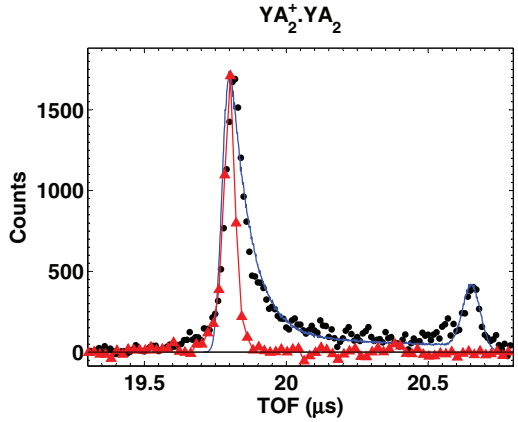

FIG. 3. TOF spectra of the neutrals formed by photodissociation of $YA_2^+\cdots YA_2$ recorded with $V_{spec} = -2.5$ kV (dots). The TOF spectrum of the same dimer with $V_{spec} = 0$ (triangles) is displayed with a shifted time-scale for comparison. Solid lines are Monte-Carlo simulations discussed in the text.

III. COMPUTATIONAL DETAILS

Minimum energy and transition state structures along the fragmentation pathway of the YA^+ dipeptide were determined using density functional theory (DFT) within the PBE0 functional and correlation consistent aug-cc-pVDZ basis set. A vibrational analysis in the harmonic approximation was carried out at each stationary point to validate its type as well as to calculate the zero point energies (ZPE). The intrinsic reaction coordinate pathways were found for each of the saddle points to check their appropriateness in connecting the particular minimum-energy structures on the multidimensional potential energy surface. The geometry optimization at the DFT level was followed by the single-point energy calculations within the MP2/aug-cc-pVDZ method.

A number of structures of the YA cation dimer with different hydrogen-bonding patterns were found within the PBE0/(aug)-cc-pVDZ approximation with a basis set augmented with diffuse functions on the hetero-atoms. Two nearly iso-energetic lowest energy structures shown in Fig. 4 were used for the following calculations. The $YA^+\cdots YA$ dimer can exist in two isomeric forms, where the proton is located either at one monomer unit or at the other. The energy barrier along the path for the interconversion of the isomers mediated by the proton transfer through a hydrogen bond is less than 2 kcal/mol. A shallow two-well potential restricts the proton location. The one-dimensional vibrational energy spectrum for this mode is close to that of a particle in the infinite potential well. The eigenvalue and eigenfunction problem for a proton inside the asymmetric two-well potential with a low barrier was recently solved in a fully quantum

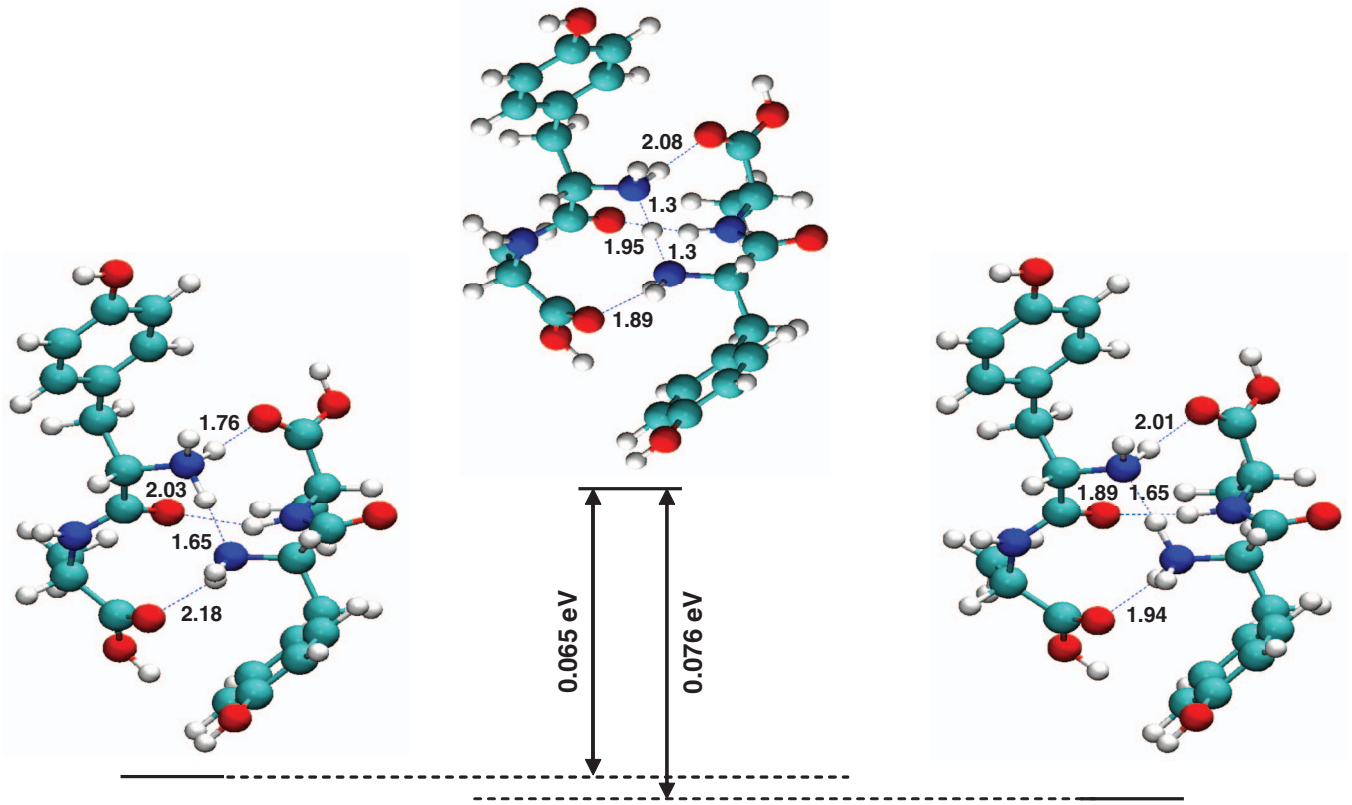

FIG. 4. The lowest-energy structures of the $YA^+\cdots YA$ dimer isomers and their interconversion transition state. H-bonds are shown as dashed lines marking their lengths in Angstroms. The MP2/(aug)-cc-pVTZ energy barriers are also shown. Green, blue, red and white balls refer to the carbon, nitrogen, oxygen and hydrogen atoms, respectively, in the ball-and-stick representation of molecular structures discussed throughout the paper. The chemical structure of the dimer is depicted in Fig. 1.

mechanical manner for the case of a model Green Fluorescent Protein chromophore with a strong intramolecular hydrogen bond.[42] The probability function for the proton location at low vibrational levels depends on an interplay between the zero point energy and the barrier height. In the asymptotic case of a negligible energy barrier, the maximum probability density, even at the zero vibrational level, corresponds to the vicinity of a transition state along the interconversion path. In the case of the YA cation dimer, the barrier could have a slight impact on the proton location at low levels, however, the conversion proceeds on a *ps*-time scale after one-photon absorption which heats up the system up to a microcanonical temperature of 809 K. Two-photon absorption leads to an even higher temperature of 1174 K. In other words, the proton is equally shared by two monomer units. Remarkably, an effective C_2 local symmetry of the geometry configuration at the transition state is higher than that of each minima. Therefore, the dimer dissociation which breaks apart the system into two subunits (accompanied by a cleavage of hydrogen bonds) has two equivalent pathways. From symmetry consideration it introduces a factor of 2 in the RRKM rate constant expression. The dimer binding energy was evaluated using the single-point energy calculations at the MP2/(aug)-cc-pVTZ level of theory with the total number of basis functions being equal to 1995. The counterpoise corrected value of the binding energy was used to eliminate the basis set superposition error (BSSE).

The photo-fragmentation lifetimes of the YA^+ dipeptide and YA cation dimer were then estimated using the RRKM/QET (quasi-equilibrium theory) microcanonical unimolecular rate constants based on quantum chemical calculations. The average lifetime equals the inverse of the rate constant for unimolecular dissociation processes. Strictly speaking, an *effective* rate constant is used if the fragmentation mechanism involves a number of elementary stages. The RRKM/QET rate constant is given by the following expression:

$$k = \frac{\sigma}{h}\frac{W^{\ddagger}(E - E_0^{\ddagger})}{\rho(E)}, \qquad (1)$$

where $W^{\ddagger}$ is the sum of energy levels at the transition state, ρ is the density of states for the reactant, $E_0^{\ddagger}$ – the activation energy including ZPE corrections, σ – the symmetry or degeneracy factor, and h is Planck's constant. The total internal energy available to the system (E) was estimated as a sum of vibrational energy of the monomer, 0.41 eV, or the dimer, 0.93 eV, at 298 K and the energy of one or two 266 nm photons (4.66 eV) depending on the experimental conditions. The exact sums and densities of harmonic oscillator eigenstates were calculated using the direct count algorithm of Beyer and Swinehart.[43]

The rate constants along the photo-induced monomer fragmentation pathway were calculated straightforwardly

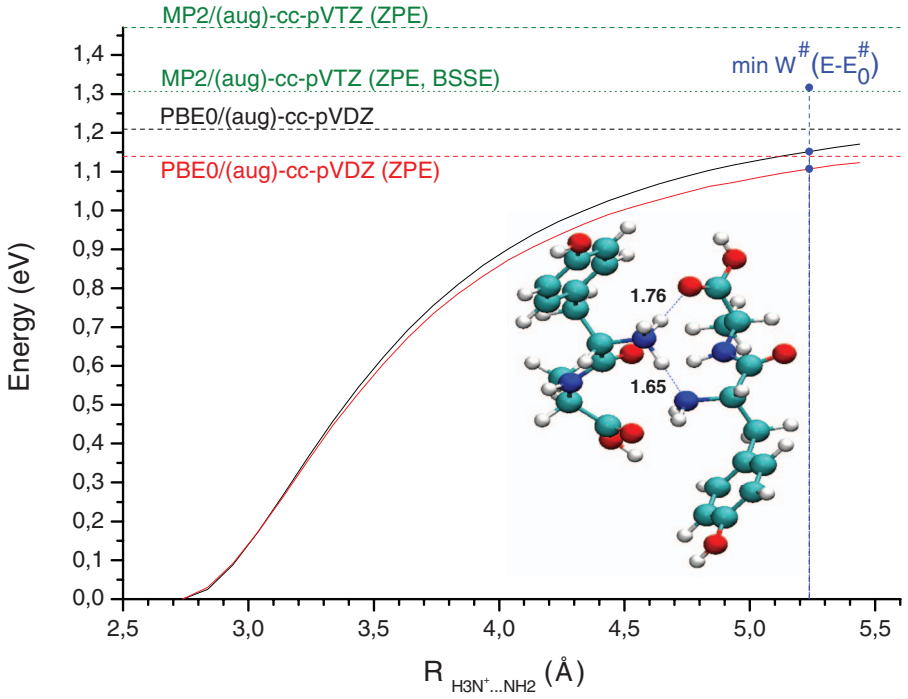

FIG. 5. The potential energy scan along dissociation of the dimer into two monomers. The internuclear separation between two nitrogen atoms of different subunits along one of the hydrogen bonds is shown. The structure corresponds to one of the true lowest-energy minima for the dimer. Two H-bonds are shown as dashed lines marking their lengths in Angstroms. The pseudo transition state is marked with the blue dots.

based on the density of states of excited reactants and the energy level sums at the transition states. The lowest energy conformer was used as a starting point in the calculated dipeptide dissociation pathway. The structure of the conformer found in the present work agrees well with the structure previously reported in conformation-specific infrared and ultraviolet spectroscopy studies of tyrosine-based protonated dipeptides and designated there as *anti*/*anti*.[44] However, the dimer photodissociation path leading to its breaking apart into two monomers, does not exhibit a distinct transition state (as in the case of a barrierless simple-bond cleavage described for example by the Morse potential). Therefore, we adopt a microcanonical variational transition state theory (VTST) approach previously applied to the calculation of the dissociation rate constant of the hydrogen fluoride and water dimers, and described in detail in Refs. 45 and 46. According to this approach, the reaction bottleneck refers to the point along the reaction path where the total number of states has a minimal value. As an initial step, the one-dimensional geometry-relaxed scan was constructed along the pathway of simultaneous cleavage of the two most strongly bound hydrogen bonds, both formed by the protonated amino group bearing a positive charge (see Fig. 5). The starting geometry shown in Fig. 5 refers to one of the true minimum energy structures. The dashed lines correspond to the binding energies of the YA cation dimer calculated at different levels of theory. The highest MP2/(aug)-cc-pVTZ level of theory with the ZPE and BSSE corrections gives a binding energy of 1.31 eV. A location of a pseudo transition state in a bond-cleavage process requires the calculation of the total number of states at each point of the potential energy curve. The pseudo transition state found for the dissociation of the YA cation dimer corresponds to the H_3N^+–NH_2 intermolecular separation being equal to 5.2 Å. Remarkably, the DFT and single-point MP2 energy curves reproduce the same geometry configuration for the pseudo transition state along the dissociation pathway, i.e., the same intermolecular separation. The relative energy of this point with respect to that of the equilibrium energy structure is very close to the predicted values of the binding energy at both levels of theory. A larger deviation is seen for the MP2 method with the extended basis set, but the BSSE corrected value eliminates the overestimation of the binding energy when calculated as a difference between energies of a dimer and two monomers calculated separately within their own basis sets. On the other hand, the BSSE-corrected values usually tend to underestimate the binding energy, which is also seen in the present case. The final MP2 energy of 1.316 eV for the pseudo transition state is somewhat higher than the one predicted at the infinite separation of the two monomer subunits including the BSSE correction.

Two issues in the estimation of dissociation rate constants in the relatively large hydrogen-bonded complexes have to be addressed. A large number of local minimum energy structures with different hydrogen-bonding, i.e., folding patterns, are found while performing partial geometry optimizations along a particular reaction coordinate. A construction of the true minimum-energy path leading to an infinite separation of two monomers requires multidimensional potential energy surface scans. To avoid extremely extensive calculations, only the bottleneck in the dimer dissociation path determined by the most strongly bound H-bonding pattern is considered in the present work. Furthermore, the pseudo transition state is obtained along the coordinate which is simply a linear

combination of the two intermolecular distances, $H_3N^+\cdots NH_2$ and $H_3N^+\cdots OC(OH)$, with equal weights. Therefore, two constraints are introduced which may result in the pseudo transition state of the second order. Indeed, the geometry configuration found in the present work exhibits two imaginary frequencies. A more thorough search of a pseudo transition state of the first order with only one negative curvature would lower the energy and add an additional degree of freedom to counting the total number of states, and thereby increase the rate constant. Our estimated value serves as a lower-bound to the rate constant, and hence defines an upper limit of the dimer lifetime implying the complete energy randomization over all the internal degrees of freedom before the dissociation. On the other hand, the anharmonic RRKM rate constants can be significantly lower by several orders of magnitude than those calculated in the harmonic approximation[46] but only in the limit of high total internal energies available in the system. An overestimation of harmonic rate constants is caused by an incorrect infinite energy spectrum of the harmonic oscillator at high energies with equally-spaced levels. It results in a great overestimation of the total number of states. The anharmonic oscillator has a correct asymptotic behavior, and a finite number of increasingly denser energy levels account for bond cleavage after the dissociation energy is reached. The true constant asymptotic behavior with respect to the total energy refers to the situation in which the system crosses the reaction barrier with a frequency of the stretching bond to be cleaved. Such an insensitivity of the rate constant to the excess of energy available in the system at the transition state is encountered at different thresholds depending on the number of degrees of freedom in the system or its microcanonical temperature, and the asymptotic lifetime is of the order of picoseconds. However, harmonic and anharmonic rate constants are usually close to each other below a certain threshold value of the total energy.[45,46] The experimental dissociation lifetimes measured in the present work range from hundreds of ns to μs, thus justifying the use of the harmonic approximation in the calculation of the RRKM rate constants at total energies well below a threshold. The only major source of errors from the neglect of anharmonic corrections is expected in the treatment of the cleavage of the weakly bound hydrogen bonds, i.e., the reaction coordinate itself. However, an anharmonic consideration would slightly reduce the rate constant by increasing the density of states of the reactants with the same total energy. Therefore, a counterbalancing effect is foreseen in estimating dissociation lifetimes of the dimer, when the pseudo transition state of the second order and the harmonic approximation are used.

For all *ab initio* calculations the FIREFLY quantum chemistry package,[47] which is partially based on the GAMESS (US) source code,[48] was used.

IV. RESULTS AND DISCUSSION

A. Time-of-flight measurements

Figure 3 shows the TOF spectrum of neutral fragments formed by UV photodissociation of $YA_2^+\cdots YA_2$ in the case where $V_{spec} = -2.5$ kV. For comparison the TOF spectrum recorded with $V_{spec} = 0$ (thus no lifetime influence on the TOF) is displayed with a shifted time-scale. The finite width of the peak in the TOF spectrum with $V_{spec} = 0$ is due to kinetic energy release during fragmentation, the finite interaction volume, and fluctuations (ripple) in the acceleration voltage. The kinetic energy release was estimated to be in the order of a few tens of meV. A comparison of the TOF spectra recorded with $V_{spec} = 0$ and -2.5 kV shows the presence of two dissociation lifetimes. The peak about 19.8 μs corresponds to a fast component while the tail leading to the peak at 20.65 μs indicates a slow dissociation component in the TOF spectrum. The peak at around 20.65 μs corresponds to neutral fragments formed between the exit of the spectrometer and the entrance of the ion-beam deflector where the ions move with constant velocity and hence have the same flight time to the MCP detector.

In Fig. 6, we compare the TOF spectra of the monomer and the dimer of YA_2^+, recorded with $V_{spec} = -2.5$ kV. Evidently, the TOF spectrum of the YA_2^+ monomer does not show a peak corresponding to (late) fragmentation outside the spectrometer. Apparently, the delayed component is related to the size of the peptide.

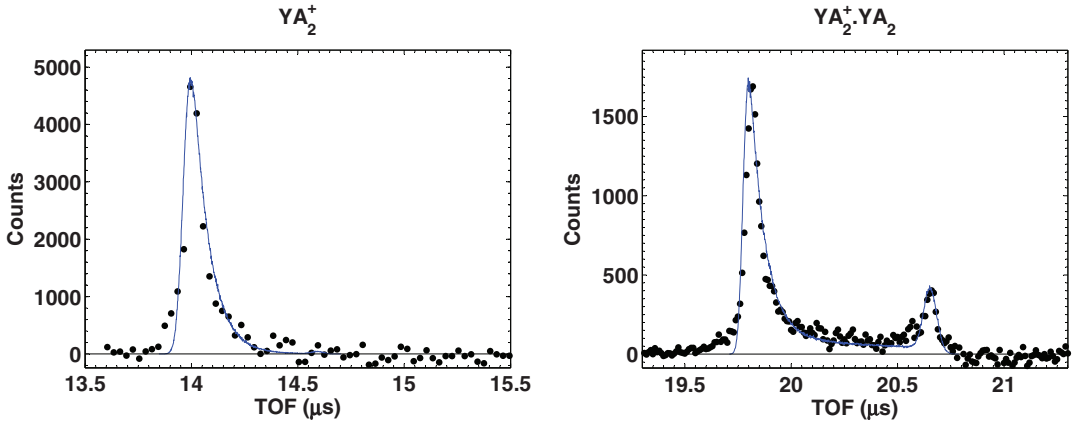

FIG. 6. TOF spectra of neutral fragments formed by photodissociation of YA_2^+ and its dimer, recorded with $V_{spec} = -2.5$ kV. Solid lines are Monte Carlo simulations for the TOFs.

B. Monte-Carlo simulation

As discussed above, the recorded TOF spectra indicate the presence of a fast and a slower dissociation channel. The associated dissociation lifetimes were determined through a Monte-Carlo simulation technique.[40] The simulation generates random dissociation events within a finite interaction volume considering the kinetic-energy release, the spread in parent-ion energy, and the laser-beam width. The neutral-fragment ejection was assumed to be isotropic. The TOF spectra were reconstructed with random dissociation events and two exponential dissociation lifetimes were adjusted to fit the deduced decay spectra.

The simulations are shown together with the data in Figs 3 and 6. For the YA_2^+ dimer the simulation yields a fast dissociation component of 195 ns and a slow dissociation component of 2.2 μs. It was established that the dimers, as a major fragmentation channel, have a positively charged monomer (see also Fig. 7) corresponding to the cleavage of the bridging H-bonds. The simulation for the YA_2^+ monomer shows only a prominent fast dissociation component with a lifetime of about 210 ns. The results of the simulations are summarized in Table I.

C. Laser-power dependence measurements

It is striking that the time scale of all fast components are of the order of 100–200 ns. A direct comparison of the lifetimes of the different peptides is however only meaningful if they involve absorption of an equal number of photons (order). To investigate this, laser-power dependence measurements were carried out both in Aarhus and in Lyon. The measurements in Lyon provided the order of the processes yielding given charged fragments, while the Aarhus measurements gave the order of absorption for the dissociations belonging to the observed slow (ca. 2 μs) and fast (ca. 100–200 ns) lifetime components.

TABLE I. Summary of the Monte Carlo simulations for dissociation lifetimes for the cationic peptides. The error bars are based on a judgement of the reproducibility of the TOF data.

Cation	τ_{slow}(ns)	τ_{fast}(ns)
YA^+	–	105 ± 10
YA_2^+	–	210 ± 20
$YA^+ \cdots YA$	1800 ± 200	175 ± 20
$YA_2^+ \cdots YA_2$	2200 ± 200	195 ± 20

The measurements show that the formation of the main iminium cation daughter fragment (mass 136 amu; a^+ or a_1^+ cf. Fig. 1) from the YA^+ and YA_2^+ monomers is due to a one-photon process. In the case of dimers, the formation of daughter monomers (ca. 2 μs) was also observed to be due to one-photon absorption while the formation of lighter fragments, such as a^+ (136 amu), was due to multi-photon absorption. The situation for the YA dimer is illustrated in Fig. 7 where mass 136 amu only appears at intense illumination.

The fast component observed for dimers is due to multi-photon excitation, which gives a higher internal microcanonical temperature of the ions after excitation and hence a faster decay. The observation of a fast multi-photon excitation (within one laser pulse) may result from simultaneous excitation of the two tyrosine chromophores. On the other hand a single tyrosine chromophore in the dimer could also absorb two photons from a single laser pulse. The absorption of the second photon could be preceded by a fast internal conversion. The strong increase in energy then results in fragmentation of one of the monomers, while only dissociation of the whole complex is observed at lower laser energy (single-photon excitation).

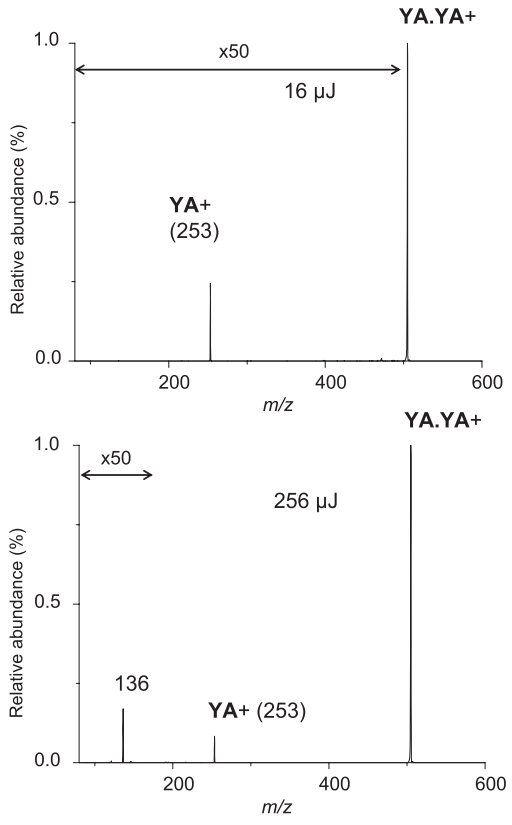

FIG. 7. Mass spectra of fragments formed by single laser shot photodissociation of $YA^+ \cdots YA$ at 266 nm with 16 μJ (upper) and 256 μJ (lower) laser-pulse energy.

D. Fragment-ion mass analysis

The fragment ion masses obtained after 5 laser pulses of 850 μJ energy are shown in Fig. 9. The main fragmentation for YA^+ is the formation of the NH_2^+=CH-CH_2-Ph-OH iminium cation (136 amu), also detected by Stearns *et al.*.[44] We consider this stage to be rate-determining in the fragmentation kinetics. It is worth noting, that the fragmentation pattern of the YA^+ dipeptide monomer has been found to be conformation-dependent when studied at low initial ground-state temperatures.[44] The energy difference between two low-energy conformations designated as *anti* and *gauche* has been found to be very small, and the loss of the tyrosine side chain radical accounts for one third of all photo-fragments in the case of the lowest-energy conformer, while this channel becomes negligible for the higher energy conformer. This channel is attributed to the direct excited-state dissociation through

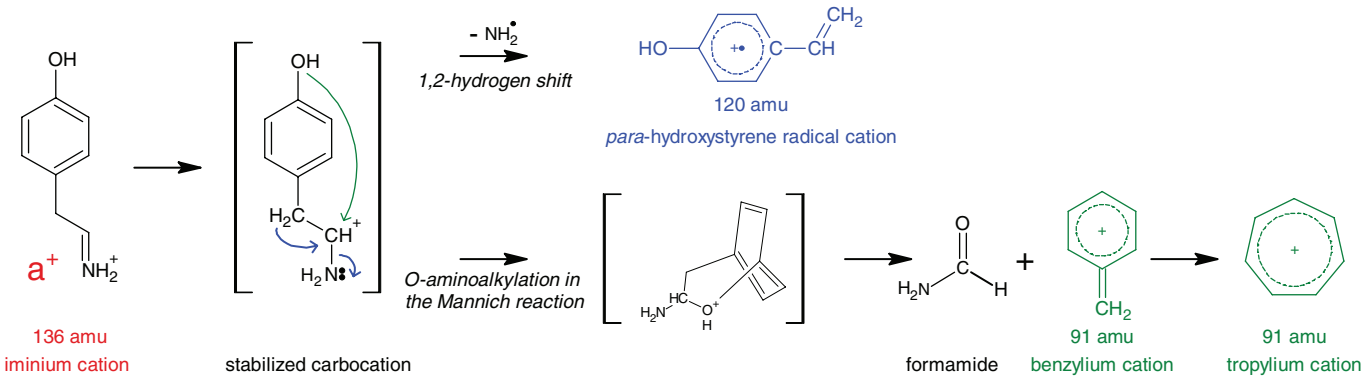

FIG. 8. Secondary processes following the a^+ formation.

a coupling to an excited state of π–σ^* character. However, there is no evidence neither for any prompt channels, nor for the loss of mass 107 amu as a major channel of fragmentation in the present study at room temperature. This clearly indicates that there is a subtle interplay between the internal conversion and direct fragmentation channels in the excited state for the YA^+ dipeptide. Presumably, there is a barrier in the excited state which separates the minimum near the Franck-Condon point on the excited state surface from the conical intersection leading to fast and efficient internal conversion. The internal energy which resides in vibrations in the ground state at room temperature is enough to overcome the barrier in the excited state. Indeed, previous *ab initio* studies of the excited state deactivation pathways of the protonated tyrosine aminoacid reveals a barrier of roughly 0.1 eV for proton transfer to the phenyl moiety in the excited state, which leads to the internal conversion to the ground-state.[49]

Two other fragments (120 amu and 91 amu) are formed in the secondary processes following a^+ formation. Mass 120 amu results from loss of the NH_2 radical from the iminium cation. The carbocation which is then formed undergoes a fast rearrangement through the 1,2-hydrogen shift (see Fig. 8) leading to formation of the *para*-hydroxysterene radical cation. This radical cation represents an ionized, entirely π-conjugated system of hydroxysterene stabilized by delocalization of both the positive charge and the radical throughout the entire system. This species no longer bears a carbocation character and is chemically more inert. Mass 91 amu may come from loss of a formamide molecule and cleavage of the side chain to yield the $C_7H_7^+$ nonradical cation (see Fig. 8).

The two most stable structural isomers of $C_7H_7^+$ are tropylium and benzylium. The former is a highly stable monocyclic aromatic hydrocarbon ring which perfectly fulfills the Hückel rule. The latter isomer is only slightly higher in energy by 0.2–0.5 eV.[50] We can not distinguish between isomers in the present work given only the daughter-masses of secondary fragments. Furthermore, mechanistic details of mass 91 amu formation have to be unraveled to describe the primary products in cleavage of the iminium cation. Presumably, the benzylium cation is formed as a first step followed by an unimolecular isomerization to the lowest-energy fully aromatic structure of tropylium. Such a conversion is governed by the residual energy available in the system to overcome the activation barrier which is estimated to be ca. 3 eV.[50] Recently recorded electronic absorption spectra in neon matrices of both isomer cations[50] could provide a possible reference for identification of these secondary products formed in the gas phase. The first step in the a^+ cleavage on the way to $C_7H_7^+$ formation is initiated by the chemical reactivity of iminium which represents a carbocation stabilized by an electron lone pair of the NH_2 group. It is a perfect reagent in the aminoalkylation of different species with a mobile proton in the Mannich reaction. Although the reaction usually proceeds with the formation of a Mannich base at the *ortho*-position of the phenol ring in solution, *O*-aminoalkylation of alcohol possibly competes with it in the gas phase depending on the strength of two nucleophilic centers and steric hindrance in the formation of an intermediate ring. The high energy-transient bicyclic structure with partially broken conjugation cleaves to form a highly stable aromatic cation and formamide. Noteworthy, all secondary fragments are of an aromatic character stabilized by a delocalization of a positive charge. Furthermore, analysis of the secondary daughter masses provides the first experimental evidence that the fragmentation of the tyrosine-containing peptides possibly results in forming the monocyclic aromatic hydrocarbon $C_7H_7^+$ of mass 91 amu and formamide. Interestingly, the formamide molecule is a highly abundant species in space (see, for example, Ref. 51). Tropylium cation has also been observed in the cometary dust.[52] Given a high enough concentration of both molecules, for example on grain surfaces, one might speculate that the back reaction can occur, resulting in formation of a close predecessor of the tyrosine aromatic aminoacid in space.

Figure 9 shows that as the size of the monomer cations increases, the formation of mass 136 amu is found to be less preferred compared to fragmentation at bonds farther away from the aromatic site (hence the appearance of heavier charged fragments). The daughter mass spectrum of the YA_2^+ tripeptide reveals more fragments compared to that of the dipeptide. Dominating fragments are formed due to the cleavage of one or the other peptide bonds along the common a_x–y_z and b_x–y_z fragmentation pathways. The fragmentation chemistry of the protonated peptides has been reviewed in Ref. 53. The daughter masses 136 and 207 amu are both iminium cations formed as a result of the cleavage of the first or the second peptide bond along the $a_{1(2)}$–$y_{2(1)}$ path and

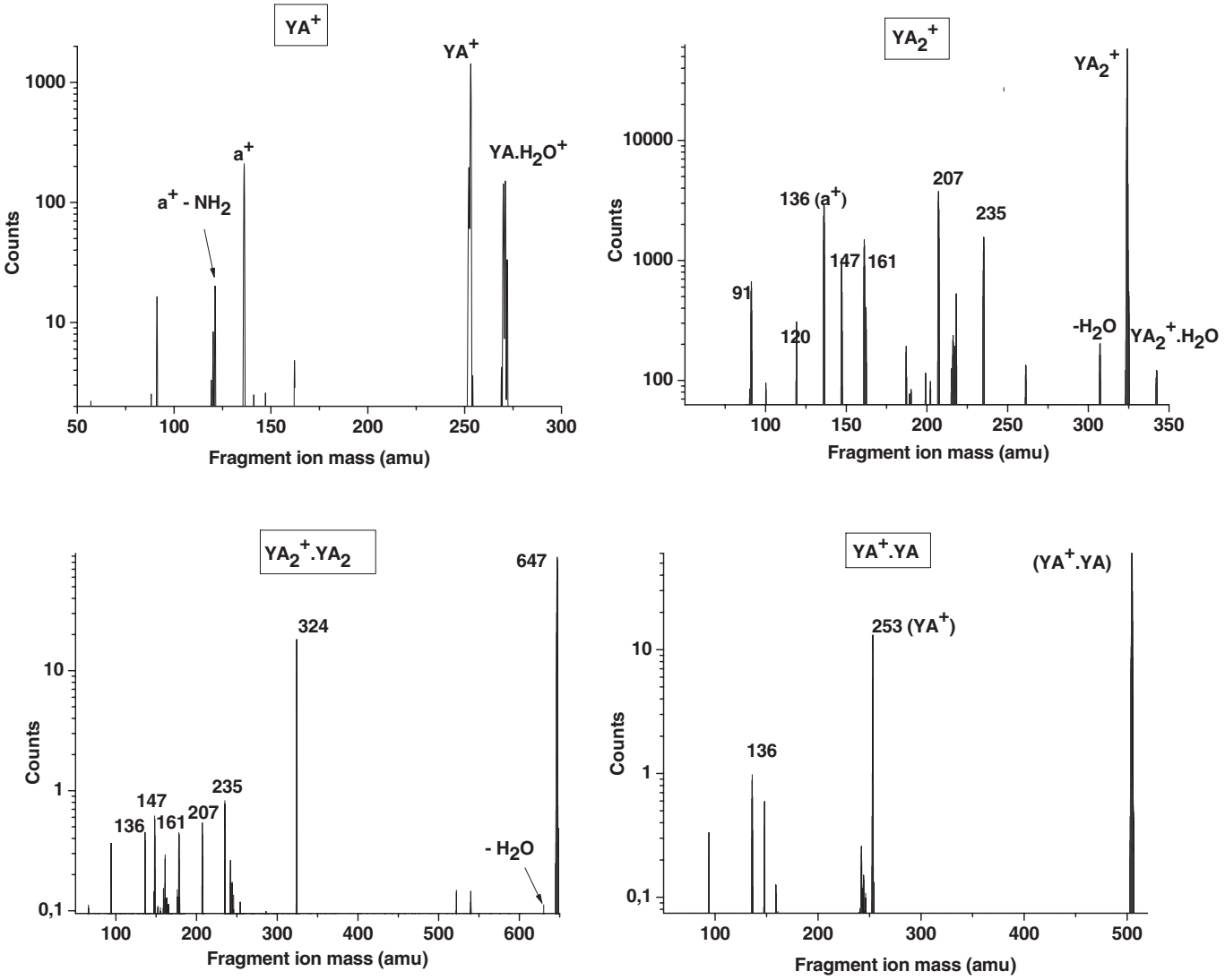

FIG. 9. Fragment-ion masses formed by photodissociation of YA_n^+[n = 1, 2], $YA^+\cdots YA$, and $YA_2^+\cdots YA_2$ at 266 nm.

designated as a_1^+ and a_2^+, respectively (see Fig. 1). The y_2 and y_1 stand for their neutral dialanine and alanine counterparts, respectively. Mass 161 amu is also formed along the a_1–y_2 channel but the charged fragment corresponds to the protonated dialanine AA^+ referred to as y_2^+. This charged fragment is formed due to the proton transfer from the iminium cation to the alanine dipeptide through a hydrogen bond between products of a cleaved tripeptide. Finally, mass 235 amu refers to the b_2^+ cation formed along the b_2–y_1 fragmentation pathway. The y_1^+ cation represents a protonated alanine A^+ aminoacid of mass 90 amu. However, its formation is less preferred due to the smaller size compared to that of the b_2^+ protonated oxazolone derivative or the a_2^+ iminium cation.

Dimer cations predominantly yield daughter monomers. It is seen that fragment ions formed in the decomposition of the monomers were also observed when their corresponding dimers were intensely illuminated (here with five laser-shots). Most likely this is mainly caused by a two-photon absorption by each of the monomer units of the dimer and then dissociation followed by fragmentation of the monomer.

E. Dissociation mechanisms

We summarize the experimental findings for the peptide dimers as follows:

1. One-photon absorption produces two peptide monomers with a lifetime of ca 2 μs. The $YA^+\cdots YA$ dimer decays faster than the bigger $YA_2^+\cdots YA_2$ dimer.
2. Two-photon absorption gives peptide fragments similar to those from the monomers. This happens on the ∼200 ns time scale.
3. There are no signs of prompt dissociation. A prompt dissociation would lead to a distinct peak of time-width in the order of 1 or 2 ns – taking the interaction volume and spread in the ion-kinetic energy into consideration (See for example Ref. 54). We do not see a distinct peak corresponding to the same in our TOF spectra.

For the monomers we have the following:

1. There is only one 100–200 ns decay channel for YA^+ and YA_2^+ which is due to one-photon absorption.

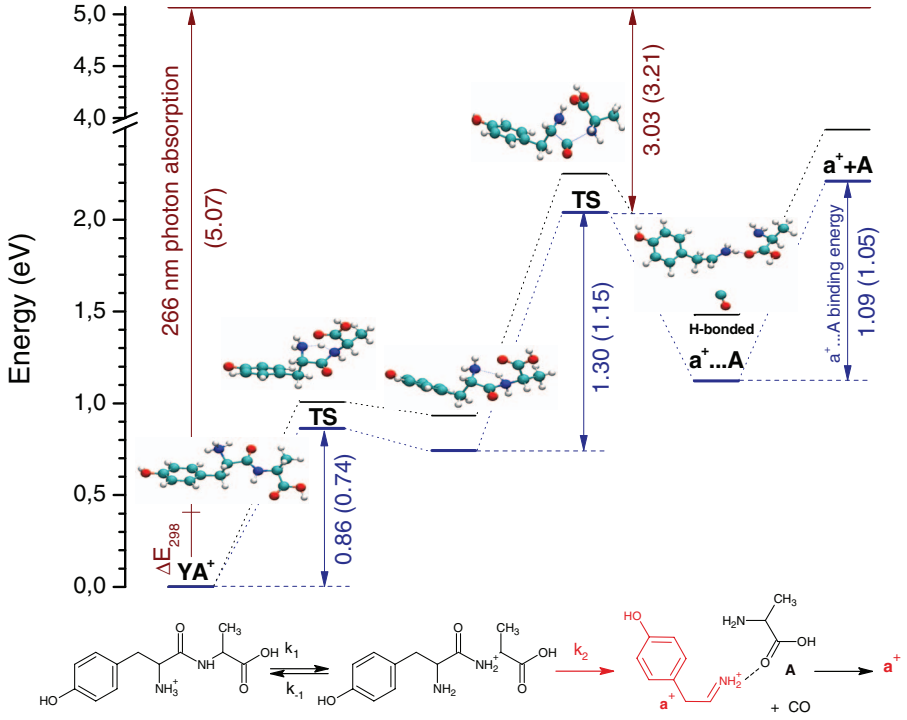

FIG. 10. Energy profile along the YA^+ fragmentation pathway. The relative energies are shown in eV. The MP2 and PBE0 results are displayed in blue and black, respectively. Total energies available at the reactant and transition state of the rate-limiting step are depicted in red. Zero point energy corrections are included into the values shown in parenthesis.

2. Among the dominating charged fragments is mass 136 amu for YA^+ (a^+) and YA_2^+ (a_1^+). This fragment is formed along the common a_1-y_z fragmentation pathway.
3. There are no signs of prompt dissociation.

The internal energy per vibrational mode after *two-photon* absorption in the dimers is about the same as the internal energy per vibrational mode in the monomers after *one-photon* absorption (the energy gain is doubled for two-photon absorption, the initial energy before photoabsorption is relatively small compared to the photon energy, and the number of normal modes in the dimer is approximately twice as large as in the monomer case). The fact that the 2-photon lifetime (∼200 ns) in the dimer is about the same as the 1-photon lifetime in the monomer indicates a statistical, ergodic origin of the observed fragmentations.

Support in this direction is also found in the work by Lucas *et al.*[22] who observed dissociation lifetimes of about 100 ns for a tripeptide, similar in size to YA_2^+. This was consistent with RRKM calculations which imply complete energy randomization over all the internal degrees of freedom before fragmentation. Moreover, we observe an increased dissociation lifetime for the YA_2^+ peptide compared to that of YA^+ and likewise for the dimers.

The fact that the formation of a^+ (intra-peptide fragmentation) disappears for one-photon excitation of the dimer strongly suggests that energy efficiently flows through the H-bonds between the two monomer peptides thus yielding a lower microcanonical temperature of the dimer.

In order to support these experimental findings, in particular the statistical nature of fragmentation in the dipeptide monomers and dimers, we have estimated their dissociation lifetimes based on *ab initio* RRKM rate constants. The main fragmentation pathway of the YA^+ monomer found in the present study, as already discussed, is the formation of the iminium cation of mass 136 amu. It results from a simultaneous cleavage of the amide and C^{α}–C_{amide} bonds which is a part of a common a_1–y_1 dissociation mechanism of protonated peptides.[55] As a result, the iminium cation a^+, the C-terminal alanine amino acid (A), and CO are formed. Figure 10 shows the reaction mechanism and energy diagram for each of the elementary stages in the cleavage process. The reaction is initiated by activation of the amide bond by a mobile proton of the protonated amino-group of tyrosine. The protonated amide is energetically less stable than the initial reactant. Furthermore, the back reaction is characterized by a very small energy barrier enabling a fast backward conversion. The second step can safely be assumed to be a rate-limiting step based on the overall energetics, while the first step is fast in both directions. Therefore, the total reaction mechanism can be treated in a quasi-equilibrium approximation. In particular, it means that the dissociation rate is determined by the second stage with the concentration of the protonated amide being approximately equal to the one dictated by an equilibrium at the first step.

The effective microcanonical rate constant of a complex reaction in the quasi-equilibrium approximation can be written as

$$k_{eff} = k_2 K_{eq} = k_2 \frac{k_1}{k_{-1}} = \frac{\sigma}{h} \frac{W^{\ddagger}(E_{YA^+} - E_0^{\ddagger}(TS^*))}{\rho(E_{YA^+})}, \qquad (2)$$

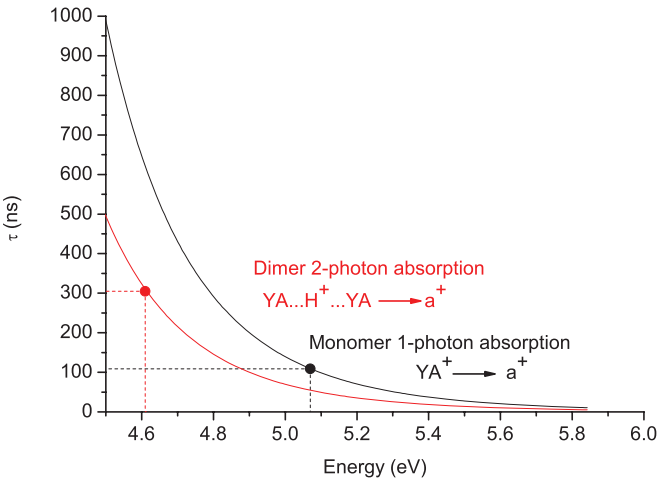

FIG. 11. Theoretical fragmentation lifetimes as a function of the total internal energy for the YA^+ dipeptide.

where $E_0^{\ddagger}(TS^*)$ stands for the excess energy at the transition state of the second elementary step, $\rho(E_{YA^+})$ stands for the density of states of the initial YA^+ dipeptide reactant, with the total available energy E. Figure 10 displays these energies in red. The symmetry factor, σ, is set to 1 for the monomer fragmentation. The calculated dissociation lifetimes as a function of the total energy E are shown in Fig. 11. The theoretical prediction of a lifetime of 109 ns for the monomer with the total energy of 5.07 eV agrees perfectly with the experimental value of 105±10 ns for a one-photon absorption of the YA^+ dipeptide cation. The total energy corresponds to the energy of one 266 nm photon added to the average internal energy of the monomer at 298 K.

Longer fragmentation lifetimes of larger peptides after one-photon absorption with the same energy can readily be understood in the frame of the RRKM theory. A qualitative description of the functional dependence of the rate constant on the size of the system, i.e., the number of vibrational degrees of freedom, leads to the following expression in the classical limit of a system of weakly bound harmonic oscillators:

$$k = \frac{1}{h}\frac{\prod_i^N \epsilon_i}{\prod_i^{N-1} \epsilon_i^{\ddagger}}\frac{(E - E_0^{\ddagger})^{N-1}}{E^{N-1}} = a\gamma(E)^{N-1}. \quad (3)$$

Here ϵ_i and $\epsilon_i^{\ddagger}$ correspond to energies of each mode for the reactant and transition state, respectively, while N is the number of active degrees of freedom. This functional form is obtained by direct analytical evaluation of inverse Laplace transformations of both the canonical partition function $Q(\beta)$ and $Q(\beta)/\beta$ expressed in terms of contour integrals.[56] Such transformations underlie the calculation of density of states ρ and the total number of states $W\ddagger$ based on the known canonical partition functions. The classical partition function for a system of N weakly bound harmonic oscillators can be written as a product of partition functions of a single oscillator $1/\beta\epsilon_i$, where β is related to the temperature T via $1/k_BT$. Thus, the rate constant depends on the fraction of excess energy in the total energy available. The power base γ is always less than unity and converges to it in the limit of high excess energy. The upper bound of the rate constant is simply equal to the ratio of products of frequencies and could also be regarded as a frequency of a bond to be cleaved assuming an absence of any change in frequencies along the fragmentation pathway except for the reaction mode. The rate constant also decreases with increasing system size. When the reaction mechanism, transition state and total energies available to the system as well as a pre-exponential factor a do not change significantly, an exponential decay of k with N can be retrieved:

$$k = ae^{-(N-1)ln(1/\gamma)}. \quad (4)$$

The exponential decay rate also depends on the excess energy, while $\ln\gamma$ is always negative. Interestingly, N is the average number of active vibrational modes simultaneously excited at a particular energy available to the system and described in the classical approximation. Strictly speaking, simultaneous excitation of all vibrational modes is practically non-reachable since the dissociation lifetimes then would be of the same order as a prompt fragmentation. The semi-classical picture corresponds to the situation in which only some of all vibrational modes can be excited at the experimental conditions, while others are not excited and do not contribute to the overall partition function due to their high characteristic temperature ($h\nu/k_B$, where ν is the frequency and k_B is Boltzmann's constant); their classical partition function is simply set to unity.

The main question is whether we are able to estimate the value of N from a theoretical point of view. The strategy used in the present study is based on an estimate of the microcanonical temperature which corresponds to the total internal energy after one-photon absorption and a calculation of an average canonical internal energy at this temperature. The number of simultaneously excited classical modes is then calculated as the ratio of an average internal energy and an average contribution to it of a single vibrational mode in the canonical ensemble, $\Delta U_{vib}/RT$, based on the equipartition theorem. Noteworthy, an application of the classical RRKM expression leads to a very good prediction of the rate constant (91 ns) in the case of the YA^+ dipeptide. The average number of active modes is equal to 50 out of a total of 99 vibrational degrees of freedom for this monomer. Note, that our classical RRKM calculations do not imply any artificial freezing of certain modes, therefore, we do not confine the phase space. An estimation of the microcanonical temperature and, hence, the number of modes simultaneously excited at a given total internal energy is based on the frequencies of all modes.

The YA^+ dipeptide monomer serves as a reference for the case of its dimer with an uncharged unit. The fragmentation mechanism of the dimer is shown in Fig. 12. As it was mentioned earlier, the dynamic structure of the dimer most likely corresponds to the situation in which the proton is shared almost equally by two monomer units; in other words the quantum mechanical probability of locating H^+ is high at the position of the transition state in the interconversion of two isomeric forms. Therefore, a degeneracy factor of 2 that reflects two symmetry-equivalent pathways in the initial dissociation of the dimer into two monomers is applied. The fragmentation proceeds if a monomer unit bears enough internal energy. It occurs after a two-photon absorption and the daughter mass-spectra clearly indicate a fragment of mass 136 amu that was

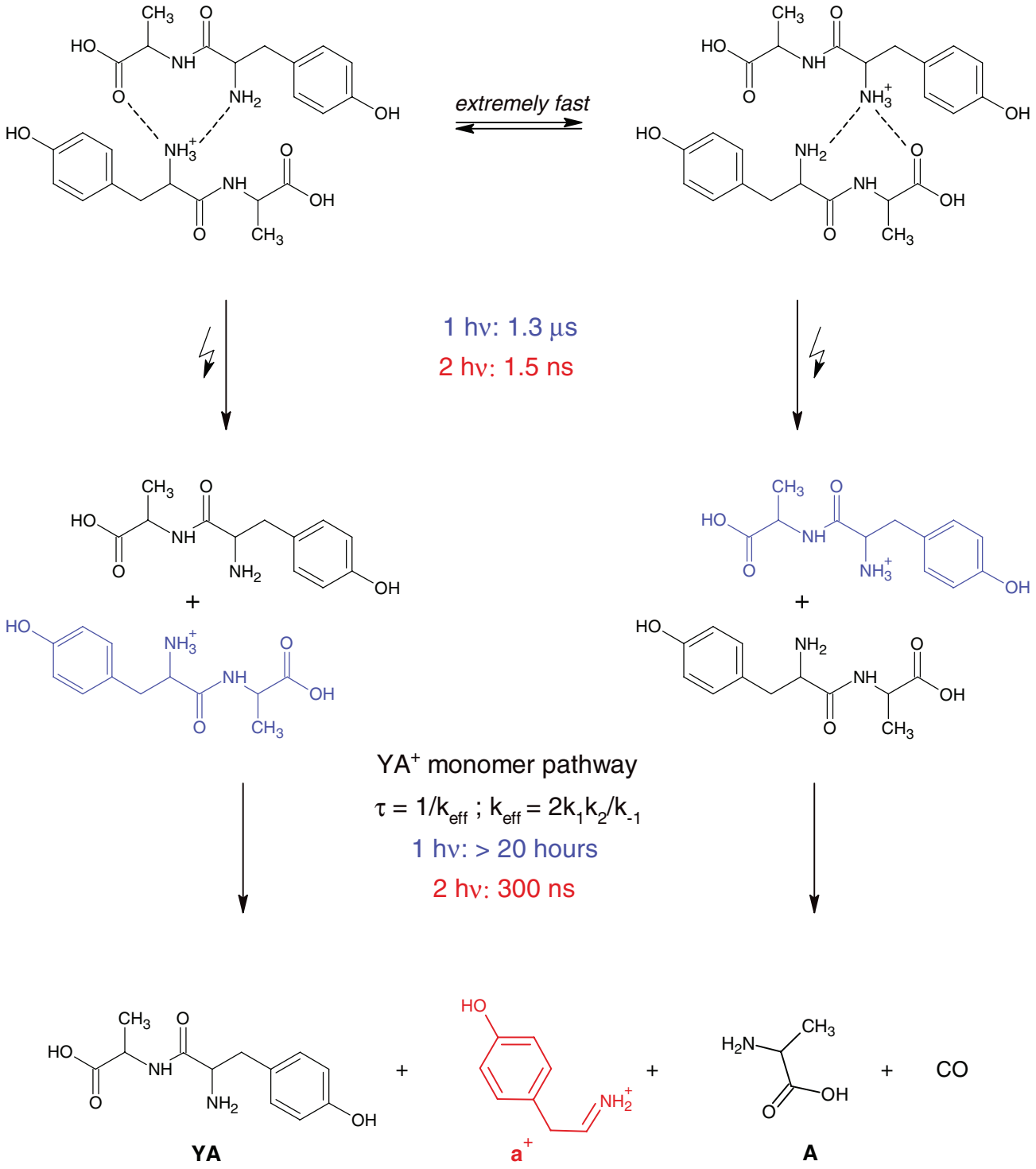

FIG. 12. Fragmentation chemistry of the $YA^+\cdots YA$ dimer cation. Two photo-induced symmetrically equivalent pathways are depicted. Lifetimes are shown for each sequential step depending on one or two-photon initial absorption.

also detected after one-photon absorption of the YA^+ dipeptide. One might have thought the reaction to proceed via a cleavage of the amide bond in the dimer, but our calculations show that this is not the case. This fact can be rationalized taking into account the energetics of two competing processes where the weaker linkage would be cleaved faster. Theoretical dissociation lifetimes of the dimer into two monomers as a function of the total energy available in the system are shown in Fig. 13. The blue and red points correspond to the experimental energies in one- and two-photon absorption, respectively. The predicted dissociation lifetime of 1.3 μs is consistent with what is observed experimentally after one-photon absorption (1.8 ± 0.2 μs). The dissociation of the dimer into two monomers proceeds on a time-scale of several ns after two-photon absorption and, thus, the limiting stage is traced to fragmentation of the monomer itself. Figure 11 shows

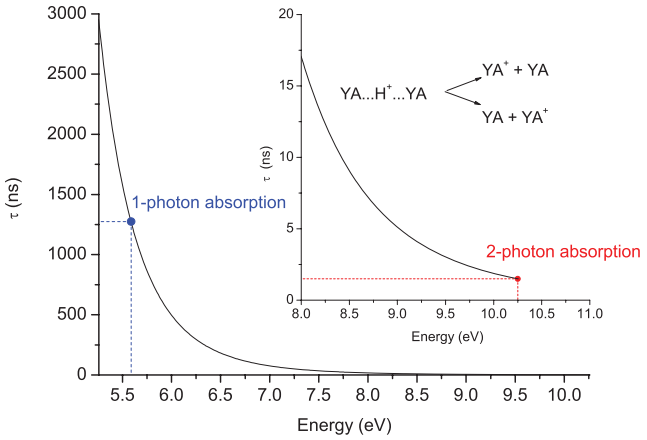

FIG. 13. Theoretical dissociation lifetimes as a function of the total internal energy for the $YA^+\cdots YA$ dimer.

results for two-photon fragmentation of the dimer yielding the iminium cation a^+. A theoretical value of 305 ns agrees rather well with the value found experimentally (175 ± 20 ns). In addition to the involvement of a pseudo transition state of the second order and the use of the harmonic approximation, the reason for a slightly larger deviation in the case of the dimer compared to the ones for the monomer may be traced to some uncertainty in determining a residual total energy of the charged monomer after the dimer dissociation. In particular, we assume an equal redistribution of the energy among two monomer units and a low kinetic energy limit for the translational and rotational degrees of freedom of monomers as a whole after cleavage of the hydrogen bonds. A slight delay in fragmentation of the dimer after two-photon absorption (175 ns), compared to that of a monomer (105 ns) after one-photon absorption, is due to the lower residual internal energy of the monomer after dimer dissociation. The difference is approximately equal to the binding energy of the dimer divided by two. A simple classical picture can also be applied to the case of the dimer two-photon fragmentation which illustrates nicely a reduction of the microcanonical temperature of the monomer formed after two-photon dissociation of the dimer, 1138 K, compared to that of the bare monomer, 1208 K. Furthermore, the decrease in the microcanonical temperature results in a slight decrease of the number of active modes by 2 which is a function of the total energy. However, the rate constant is more sensitive to changes in the power base in equation (3). The estimated classical fragmentation lifetime is equal to 301 ns being very close to the quantum prediction.

Both the quantum and the classical RRKM rate constants, based on the results of *ab initio* calculations, prove that the fragmentation of the dipeptide monomer and dimer is statistical in nature, and the decay times found in the present work are long enough for complete energy randomization, particularly, for the dimer in which the energy transfer is mediated by the hydrogen bonds.

V. CONCLUSION

Photodissociation-lifetime measurements were performed for protonated, gas-phase $YA_n^+[n = 1,2]$ peptide monomers and their dimers at 266 nm excitation by a technique based on time-of-flight in a homogeneous electric field. The fragment-ion masses were analyzed using a high resolution quadrupole-mass spectrometer. The observed dissociation lifetimes fall into two categories: a fast (~100–200 ns) and a slow (~2 μs) component. Note that both components are so short-lived that they will not survive one revolution in an ion-storage ring[57] and hence the lifetimes cannot be obtained there. Laser power dependence measurements were used to identify the occurrence of one and two-photon absorption processes. The YA^+ and YA_2^+ monomers only decay with the short lifetime in a single-photon process whereas both one and two-photon absorption occurs for the dimer systems. It is argued that both the fast fragmentation from single-photon absorption in the monomers as well as the slow single-photon reaction which cleaves the dimers into two monomers are ergodic processes. The results show that energy is easily transferred across the dimer H-bonds connecting the monomers. Since energy transport through an H-bond typically takes place on the ps-time scale, we can safely say that the H-bond mediated energy transport in the dimer is not rate limiting. *Ab initio* RRKM-based calculations strongly support the fact that the decay time of about 2 μs is long enough for complete energy randomization in the dimer-peptide cations. Furthermore, the dissociation lifetimes are fully consistent with RRKM calculations for the dipeptide monomer and dimer, which imply ergodic dissociation for both of them.

ACKNOWLEDGMENTS

We thank S. Brøndsted Nielsen for useful discussions. This work is supported by the Carlsberg Foundation, Lundbeckfonden, the Danish Research Agency and the Marie Curie European Career Integration Grant within the 7th European Community Framework Programme. A.V.B. acknowledges the support from the Russian Foundation for Basic Research (grant #11-03-01214) and from the grant MK-64815.2010.4, as well as the Research Computing Center at the M.V. Lomonosov Moscow State University for providing computing resources.

[1]N. C. Polfer and J. Oomens, Phys. Chem. Chem. Phys. **9**, 3804 (2007).
[2]J. N. Butler and G. B. Kistiakowsky, J. Am. Chem. Soc. **82**, 759 (1960).
[3]C. Lifshitz, J. Phys. Chem. **87**, 2304 (1983).
[4]D. Boyall and K. L. Reid, Chem. Soc. Rev. **26**, 223 (1997).
[5]R. A. Coveleskie, D. A. Dolson, and C. S. Parmenter, J. Chem. Phys. **72**, 5774 (1980).
[6]R. Naaman, D. M. Lubman, and R. N. Zare, J. Chem. Phys. **71**, 4192 (1979).
[7]K. K. Lehmann, G. Scoles, and B. H. Pate, Annu. Rev. Phys. Chem. **45**, 241 (1994).
[8]G. A. Worth and L. S. Cederbaum, Annu. Rev. Phys. Chem. **55**, 127 (2004).
[9]B. G. Levine and T. J. Martinez, Annu. Rev. Phys. Chem. **58**, 613 (2007).
[10]D. Polli, P. Altoe, O. Weingart, K. M. Spillane, C. Manzoni, D. Brida, G. Tomasello, G. Orlandi, P. Kukura, R. A. Mathies, M. Garavelli, and G. Cerullo, Nature (London) **467**, 440 (2010).
[11]M. Gruebele and R. Bigwood, Int. Rev. Phys. Chem. **17**, 91 (1998).
[12]M. Kordel, D. Schooss, S. Gilb, M. N. Blom, O. Hampe, and M. M. Kappes, J. Phys. Chem. A **108**, 4830 (2004).
[13]L. Joly, R. Antoine, M. Broyer, J. Lemoine, and P. Dugourd, J. Phys. Chem. A **112**, 898 (2008).
[14]K. H. Kraemer, Proc. Natl. Acad. Sci. U.S.A. **94**, 11 (1997).

[15]H. Mukhtar and C. A. Elmets, Photochem. Photobiol. **63**, 356 (1996).
[16]D. P. Little, J. P. Speir, M. W. Senko, P. B. O'Connor, and F. W. McLafferty, Anal. Chem. **66**, 2809 (1994).
[17]R. A. Zubarev, N. A. Kruger, E. K. Fridriksson, M. A. Lewis, D. M. Horn, B. K. Carpenter, and F. W. McLafferty, J. Am. Chem. Soc. **121**, 2857 (1999).
[18]L. H. Andersen, H. Bluhme, S. Boyé, T. J. D. Jørgensen, H. Krogh, I. B. Nielsen, S. B. Nielsen, and A. Svendsen, Phys. Chem. Chem. Phys. **6**, 2617 (2004).
[19]L. H. Andersen, I. B. Nielsen, M. B. Kristensen, M. O. A. El Ghazaly, S. Haacke, M. B. Nielsen, and M. Å. Petersen, J. Am. Chem. Soc. **127**, 12347 (2005).
[20]R. Antoine, M. Broyer, J. Chamot-Rooke, C. Dedonder, C. Desfrançois, P. Dugourd, G. Grégoire, C. Jouvet, D. Onidas, P. Poulain, T. Tabarin, and G. Van Der Rest, Rapid. Commun. Mass. Spectrom. **20**, 1648 (2006).
[21]I.-R. Lee, W. Lee, and A. H. Zewail, Proc. Natl. Acad. Sci. U.S.A. **103**, 258 (2006).
[22]B. Lucas, M. Barat, J. A. Fayeton, C. Jouvet, P. Çarçabal, and G. Grégoire, Chem. Phys. **347**, 324 (2008).
[23]G. Aravind, L. Lammich, and L. H. Andersen, Phys. Rev. E **79** (2009).
[24]J. A. Wyer, A. Ehlerding, H. Zettergren, M.-B. S. Kirketerp, and S. B. Nielsen, J. Phys. Chem. A **113**, 9277 (2009).
[25]L. Joly, R. Antoine, A.-R. Allouche, M. Broyer, J. Lemoine, and P. Dugourd, J. Am. Chem. Soc. **129**, 8428 (2007).
[26]C. Loison, R. Antoine, M. Broyer, P. Dugourd, J. Guthmuller, and D. Simon, Chem. Eur. J. **14**, 7351 (2008).
[27]M. Guidi, U. J. Lorenz, G. Papadopoulos, O. V. Boyarkin, and T. R. Rizzo, J. Phys. Chem. A **113**, 797 (2009).
[28]M. Perót, B. Lucas, M. Barat, J. A. Fayeton, and C. Jouvet, J. Phys. Chem. A **114**, 3147 (2010).
[29]M. T. Rodgers, S. Campbell, E. M. Marzluff, and J. L. Beauchamp, Int. J. Mass Spectrom. Ion Processes **148**, 1 (1995).
[30]M. Meot-Ner, A. R. Dongré, A. Somogyi, and V. H. Wysocki, Rapid. Comm. Mass. Spectrom. **9**, 829 (1995).
[31]R. Weinkauf, P. Schanen, D. Yang, S. Soukara, and E. W. Schlag, J. Phys. Chem. **99**, 11255 (1995).
[32]R. Weinkauf, P. Schanen, A. Metsala, E. W. Schlag, M. Burgle, and H. Kessler, J. Phys. Chem. **100**, 18567 (1996).
[33]R. Weinkauf, E. W. Schlag, T. J. Martinez, and R. D. Levine, J. Phys. Chem. A **101**, 7702 (1997).
[34]E. W. Schlag, H. L. Selzle, P. Schanen, R. Weinkauf, and R. D. Levine, J. Phys. Chem. A **110**, 8497 (2006).
[35]Y. Hu, B. Hadas, M. Davidovitz, B. Balta, and C. Lifshitz, J. Phys. Chem. A **107**, 6507 (2003).
[36]S.-Y. Sheu, D.-Y. Yang, H. L. Selzle, and E. W. Schlag, J. Phys. Chem. A **106**, 9390 (2002).
[37]L. Y. Baranov and E. W. Schlag, Z. Naturforsch. A **54a**, 387 (1999).
[38]H. Kang, C. Jouvet, C. Dedonder-Lardeux, S. Martrenchard, G. Grégoire, C. Desfrançois, J.-P. Schermann, M. Barat, and J. A. Fayeton, Phys. Chem. Chem. Phys. **7**, 394 (2005).
[39]H. B. Pedersen, M. J. Jensen, C. P. Safvan, X. Urbain, and L. H. Andersen, Rev. Sci. Instrum. **70**, 3289 (1999).
[40]L. Lammich, I. B. Nielsen, H. Sand, A. Svendsen, and L. H. Andersen, J. Phys. Chem. A **111**, 4567 (2007).
[41]V. Larraillet, R. Antoine, P. Dugourd, and J. Lemoine, Anal. Chem. **81**, 8410 (2009).
[42]J. Rajput, D. B. Rahbek, L. H. Andersen, T. Rocha-Rinza, O. Christiansen, K. B. Bravaya, A. V. Erokhin, A. V. Bochenkova, K. M. Solntsev, J. Dong, J. Kowalik, L. M. Tolbert, M. Å. Petersen, and M. B. Nielsen, Phys. Chem. Chem. Phys. **11**, 9996 (2009).
[43]S. E. Stein and B. S. Rabinovitch, J. Chem. Phys. **58**, 2438 (1973).
[44]J. A. Stearns, M. Guidi, O. V. Boyarkin, and T. R. Rizzo, J. Chem. Phys. **127** (2007).
[45]L. Yao, A. M. Mebel, and S. H. Lin, J. Phys. Chem. A **113**, 14664 (2009).
[46]L. Yao, R. X. He, A. M. Mebel, and S. H. Lin, Chem. Phys. Lett. **470**, 210 (2009).
[47]A. A. Granovsky, FIREFLY, version 7.1.G., http://classic.chem.msu.su/gran/firefly/index.html.
[48]M. W. Schmidt, K. K. Baldridge, J. A. Boatz, S. T. Elbert, M. S. Gordon, J. H. Jensen, S. Koseki, N. Matsunaga, K. A. Nguyen, S. Su, T. L. Windus, M. Dupuis, and J. A. Montgomery, J. Comput. Chem. **14**, 1347 (1993).
[49]G. Grégoire, C. Jouvet, C. Dedonder, and A. L. Sobolewski, J. Am. Chem. Soc. **129**, 6223 (2007).
[50]A. Nagy, J. Fulara, I. Garkusha, and J. P. Maier, Angew. Chem. Int. Ed. **50**, 3022 (2011).
[51]J. M. Hollis, F. J. Lovas, A. J. Remuan, P. R. Jewell, V. V. Ilyushin, and I. Kleiner, Astrophys. J. **643**, L25 (2006).
[52]J. Kissel, F. R. Krueger, J. Silén, and B. C. Clark, Science **304**, 1774 (2004).
[53]B. Paizs and S. Suhai, Mass Spectrom. Rev. **24**, 508 (2005).
[54]L. Lammich, J. Rajput, and L. H. Andersen, Phys. Rev. E **78** (2008).
[55]B. Paizs, M. Schnölzer, U. Warnken, S. Suhai, and A. G. Harrison, Phys. Chem. Chem. Phys. **6**, 2691 (2004).
[56]H. Eyring, S. H. Lin, and S. M. Lin, *Basic Chemical Kinetics* (Wiley, New York, 1980).
[57]L. H. Andersen, O. Heber, and D. Zajfman, J. Phys. B **37**, R57 (2004).